

THESIS TITLE

by

Handan Çetin

B.S., Molecular Biology and Genetics, Canakkale Onsekiz Mart University, 2018

Submitted to the Institute for Graduate Studies in
Science and Engineering in partial fulfillment of
the requirements for the degree of
Master of Science

Graduate Program in Computational Science and Engineering
Boğaziçi University

2020

TABLE OF CONTENTS

LIST OF FIGURES	ii
LIST OF TABLES	iii
1. INTRODUCTION	1
1.1. Systems Biology	1
1.1.1. Metabolic Networks	2
1.1.2. Mathematical Representation of Metabolic Networks	5
1.1.3. Flux Balance Analysis	5
1.2. <i>Saccharomyces cerevisiae</i>	5
1.2.1. Central Carbon Metabolism of <i>S. cerevisiae</i>	5
1.2.2. Metabolic Models of <i>S. cerevisiae</i>	7
1.2.3. Applications of <i>S. cerevisiae</i> GSMMs	7
1.3. Significance of Thesis	7
2. MATERIALS AND METHODS	8
2.1. Experimental Data Preparation	8
2.1.1. Data Acquisition	8
2.1.2. Determination of Rates	10
2.2. Model Selection	12
2.3. Flux Balance Analysis	14
2.4. Visualization of the Model	15
3. RESULTS	16
3.1. Intracellular Flux Distributions	16
4. DISCUSSION	18
5. EXPANDABLE TOPICS	19
5.1. Following topics can be added into introduction	19
REFERENCES	20

LIST OF FIGURES

Figure 1.1.	Systems biology approaches	2
Figure 1.2.	Overview of metabolic network reconstruction protocol	4
Figure 1.3.	Central carbon mechanism of <i>S. cerevisiae</i>	6
Figure 2.1.	OD ₆₀₀ , lnOD ₆₀₀ , cell dry weights and growth rates	11
Figure 3.1.	Non-zero fluxes in the solution	16
Figure 3.2.	Map view of the non-zero flux distributions	17

LIST OF TABLES

Table 2.1.	Measured OD ₆₀₀ and cell dry weight values of reference strain . . .	9
Table 2.2.	Measurements of extracellular concentrations	10
Table 2.3.	Calculated flux values	11
Table 2.4.	Reaction list in the iAN50 model	13
Table 2.5.	Biomass coefficients	14

1. INTRODUCTION

1.1. Systems Biology

With the increasing availability of the computational tools and the development of high throughput techniques in the omics field, systems biology has shown a strong emergence in the last few years as a key multi-disciplinary field for integrating the multi-layer complexity of biological systems, particularly in the areas of transcriptomics, proteomics, metabolomics and fluxomics [1]. This amount of available data allows researchers to investigate molecular cell processes in a large scales, applying theoretical, experimental and computational methods.

Biological systems based on complex interactions between various molecular components. The relations between these components are often obey nonlinear kinetics, for example, most of the reactions are regulated by one or more feedback or feed-forward loops with incomprehensible behaviours. When considered, cell structure and compartmentalization are also often introduce complexities to the unexpected behavior of the entire biological system [2]. Mathematical modeling with these factors taken into consideration is used as a general approach to encompass existing knowledge in biological systems, and to gather information by analyzing these models to acquire a better understanding [3].

A mathematical model of a cell can be approached by two different approaches in either a bottom-up or top-down directionality (Figure 1.1) [4, 5]. Top-down approach is an experimental oriented approach, it starts from the whole picture and aims to characterize biological mechanisms closer to the smaller parts and their interactions in the network. In the bottom-up approach, collected data from biological knowledge is used as a starting point, a subsystem is generated to deduce the functional properties of smaller points in the network. Combination of the pathway level models (bottom-up) into a model for the entire system level (top-down) is the ultimate goal in the systems biology therefore these approaches are complementary.

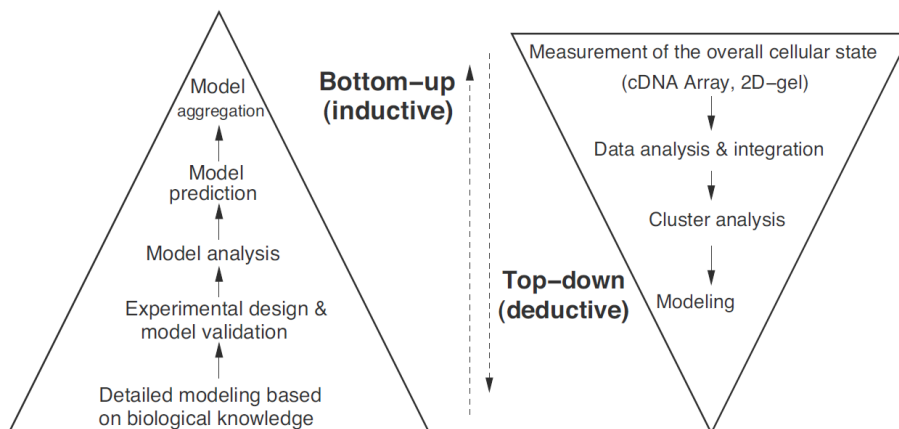


Figure 1.1. Systems biology approaches. Left: Bottom-up approach. Right: Top-down approach. Figure is taken from [3].

1.1.1. Metabolic Networks

In the context of systems biology, metabolic network reconstructions have become a common interest for the researchers over the past 20 years [6]. Organism-specific metabolic network analyses allow scientists to design experiments and even obtain beforehand predictions. These networks are the main sources of the mathematical models which can simulate metabolic fluxes reflecting the experimental reality [7].

Before the improvement of genome sequencing or annotation technologies, initial core metabolic networks were based on the accessible information of biochemical pathways [8] [9]. In the last decade, larger genome-scale metabolic models (GSMMs) have been able to be developed rapidly with the help of databases for annotated genomes, providing information on substrates and products of each enzyme and each bioreaction [10]. Growing biochemical databases provide automatization processes for the metabolic network reconstructions. As a result, genome-scale metabolic networks are available today for almost all organisms with an annotated genome available in the literature [11,12]. From the first genome-scale metabolic model of *Escherichia coli* to other organisms, the steps are required for GSMM development remained the same regardless of the biological diversity.

A generally applicable protocol is defined by the Palsson group [6, 10] for the reconstruction of biochemical networks described in the Figure 1.2 [13]. Briefly, genomic data for the biochemical reactions of an organism are identified from the databases, such as NCBI, DDBJ and EMBL-EBI. Extraction and processing of the gene-protein-reaction relationship (GPR) of the genomic data results a draft reconstruction. GPR associations in the draft model should be reviewed by the researchers and manually curated if the identifying process is achieved with the help of automated computational algorithms [11]. Since the genomic data is the least representative of the biological phenotypes, available transcriptomic, proteomic, metabolomic and/or subcellular localization data are also used to further curate the model. Once the final metabolic network is reconstructed with bibliographic information, it is translated into a mathematical model.

Once a metabolic network is reconstructed, a rational link between a genome sequence, the proteins encoded in the genome, and the reactions catalyzed by the proteins allowing to investigate the relationships between genotype and phenotype is achieved [14]. As the final step, GSMM needs to be validated by the new experimental data sets. GSMM validation process for various experimental conditions require detailed cultivation data from experiments. For example, information on the biomass composition of the specific organism leads more accurate biomass equation in the model, that is one of the key factors in the GSMM optimization and validation [15]. Even though multiple steps in the GSMM reconstruction can be achieved with the automated softwares available, it is usually necessary to curate the obtained model manually.

Approaches for analyzing metabolic networks are mainly categorized as dynamic or structural approaches. Even though the former is promising more realistic approach, its implementation in the literature is obstructed due to the unavailability of kinetic parameters for the majority of enzymes within a metabolic network [16, 17]. Because of the lack of kinetic parameters, structural metabolic modeling has been widely used for analyzing cellular metabolism at a steady-state assumption.

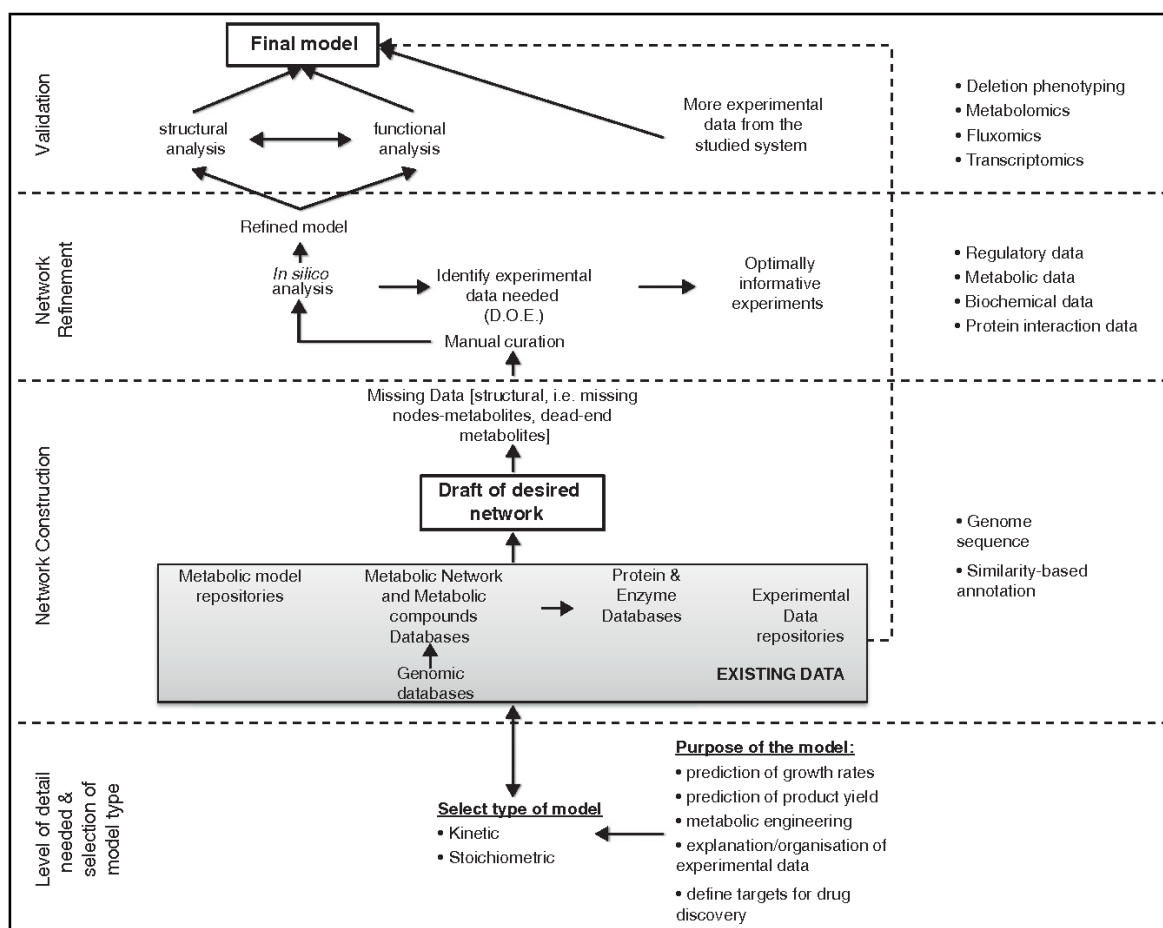


Figure 1.2. Overview of metabolic network reconstruction protocol. Figure is taken from [13].

GSMMs are one of the most useful tools in systems biology, especially in metabolic engineering studies [18]. In 1998, with the publication of *Metabolic Engineering: Principles and Methodologies*, the term metabolic engineering is defined as the optimization of natural processes within cells to increase the production of certain substances [19]. Hence, studies of metabolic engineering can be considered as genetic engineering in strain development. However, while metabolic engineering manipulates strains by altering flux distributions in the pathways; genetic engineering modifies specific genes, proteins and/or enzymes of interest [20]. Although GSMMs are mainly used in metabolic engineering strategies, other applications both for descriptive and predictive purposes can be found in the literature [21].

The ultimate goal of the GSMM reconstruction is to predict flux distribution profiles as close *in silico* as they are *in vivo*. Hence, GSMMs are in continuous research to improve predictability of organism-specific models.

Here, a figure of "GSMM citation numbers vs year" can be added from WOS

1.1.2. Mathematical Representation of Metabolic Networks

In this section, there will be a review on "Mathematical Framework Behind the Reconstruction and Analysis of Genome Scale Metabolic Models" [22], similar to slides that I've prepared for MFA.

1.1.3. Flux Balance Analysis

In this section, there will be a review on "What is flux balance analysis?" [7]

1.2. *Saccharomyces cerevisiae*

The species "yeast" includes a range of eukaryotic single-celled microorganisms, although it is commonly used to describe *Saccharomyces cerevisiae*. Also known as the baker's yeast, *S. cerevisiae* is one of the extensively used microorganisms for alcoholic fermentation of beverages, bio-ethanol production, and processing various foods since ancient times [23]. It was the first eukaryotic organism whose genome was fully sequenced and annotated [24], and besides its benefits in the industry, it is used as a model system for other eukaryotic cells including humans [25, 26].

1.2.1. Central Carbon Metabolism of *S. cerevisiae*

From the end of the eighteenth century, mainly after the fermentation is defined as "respiration without oxygen", the metabolism of *S. cerevisiae* has been studied extensively [27, 28]. Its capability to produce ethanol is one of the most characterized microbial processes due to industrial utilization.

The set of anabolic and catabolic reactions in the cell are referred as the metabolism. A schematic representation of the central carbon metabolism in *S. cerevisiae* can be found in Figure 1.3. Glycolysis, pentose-phosphate pathway (PPP), tricarboxylic acid cycle (TCA) or Krebs cycle, the glyoxylate cycle and the electron transport chain are the main pathways in central carbon metabolism.

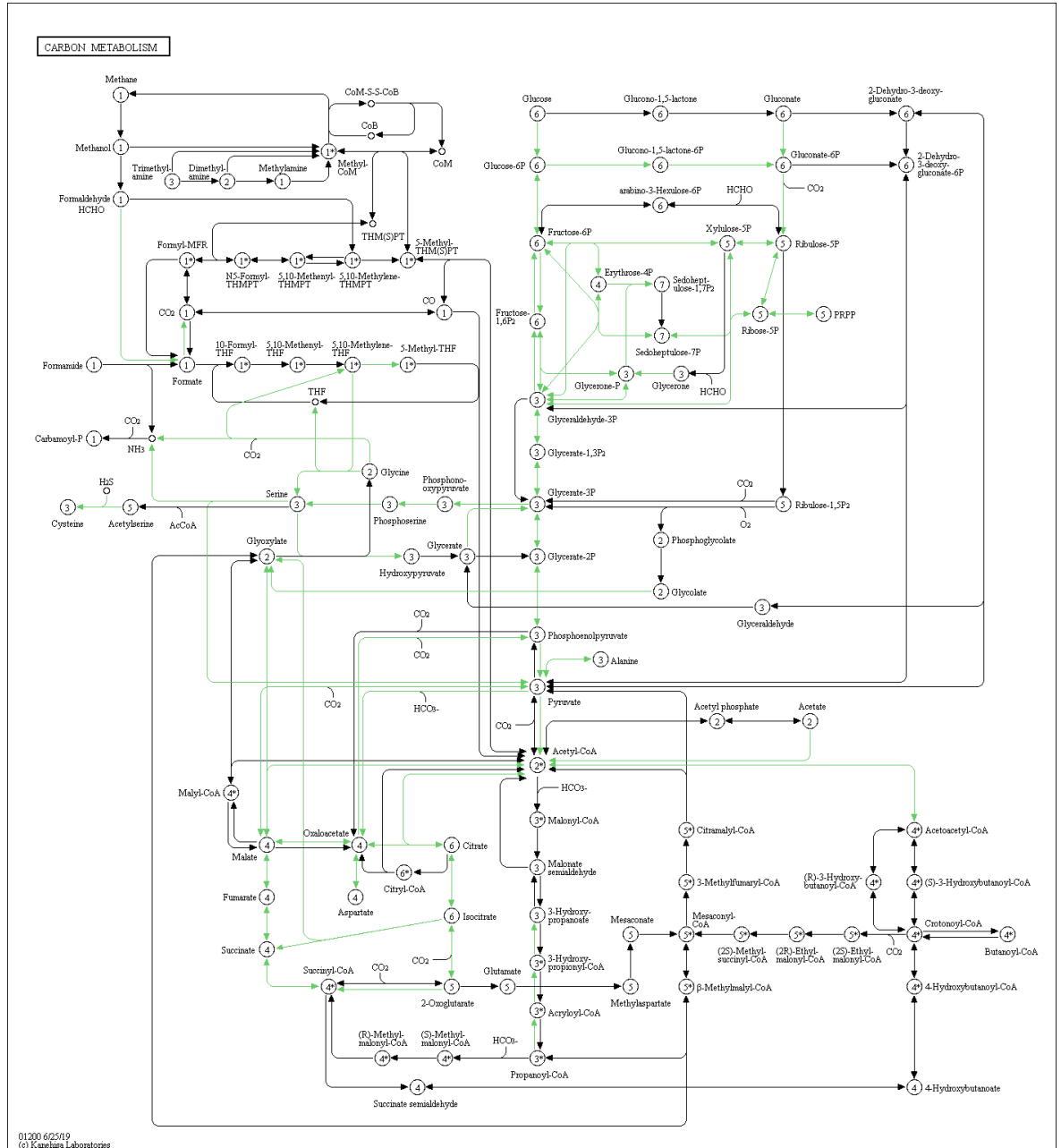


Figure 1.3. Central carbon mechanism of *S. cerevisiae* obtained from KEGG [29].

1.2.2. Metabolic Models of *S. cerevisiae*

After the first *S. cerevisiae* genome sequence is published, the first cDNA spotted microarray exploring metabolic gene regulation in 1997 [30], and the first commercial platform for oligonucleotide microarray data (Affymetrix) to investigate cellular regulations were reported in 1998 [31]. Existing genome data is integrated with the extensive annotation based on microarray data and biochemical knowledge from literature, leading of the publication of the first GSMM of *S. cerevisiae* in 2013 [32]. More in this section, there will be review on: Genome-scale modeling of yeast: chronology, applications and critical perspectives [33]

1.2.3. Applications of *S. cerevisiae* GSMMs

Literature research on the applications will be added.

1.3. Significance of Thesis

The purpose of this master's thesis is to enlighten molecular mechanisms behind the tolerance in yeast. Intracellular flux distributions of resistant strains for various substances such as caffeine, ethanol, iron, phenylethanol, nickel and sodium chloride are going to be analyzed comparatively. This study will also contribute to the global understanding of metabolic regulations in the *S. cerevisiae*, and will be further expandable into metabolic engineering studies.

2. MATERIALS AND METHODS

2.1. Experimental Data Preparation

2.1.1. Data Acquisition

Extracellular metabolomics data is obtained from Cakar’s Lab [34]. Briefly, they perform ethyl methane sulfonate (EMS) mutagenesis on the prototrophic *Saccharomyces cerevisiae* strain CEN.PK 113-7D (MATa, MAL2-8c, SUC2) to increase the genetic diversity as an evolutionary engineering selection strategy. Cells were inoculated in 2% Yeast Minimal Media (YMM), and the extracellular concentrations of glucose, ethanol, glycerol and acetate were measured at different time points. OD₆₀₀ values were determined by a spectrophotometer. Additionally, cell dry weight analysis was conducted to determine biomass production. Acquired extracellular metabolite concentrations, OD₆₀₀ values and dry weights of the reference strain (without mutagenesis) were used in this study are collected in Table 2.2 and Table 2.1.

Table 2.1. Measured OD₆₀₀ and cell dry weight values of reference strain.

Time (h)	OD600	ln(OD600)	Cell DW (g/L)
0	0.21	-1.560647748	-
3	0.53	-0.634878272	-
6	1.76	0.565313809	0.9
7.5	2.66	0.978326123	-
9	4.46	1.495148766	1.9
12	5.31	1.669591835	-
15	5.88	1.771556762	-
18	5.83	1.763017	2.32
21	6.07	1.803358605	-
24	5.87	1.769854634	-
30	6.14	1.814824742	2.26
40	6.44	1.86252854	-
46	6.36	1.850028377	-
50	6.3	1.840549633	-
54	6.55	1.87946505	-
63	6.54	1.877937165	-
67	6.88	1.928618652	-
72	6.97	1.941615225	2.66

Table 2.2. Measurements of extracellular concentrations.

Time (h)	Glucose (g/L)	Ethanol (g/L)	Glycerol (g/L)	Acetate (g/L)
0	19.99	0	0	1.08
3	17.98	0.58	0.02	1.24
6	15.85	1.2	0.06	1.16
9	12.21	3.39	0.18	1.37
12	9.18	7.97	0.61	2.45
15	0.4	8.17	0.69	2.46
27	0	8.28	0.76	2.6
46	0	8	0.77	2.45
50	0	6.62	0.64	2.02
54	0	5.74	0.55	1.73
58	0	5.46	0.54	1.74
72	0	3.72	0.49	1.33

2.1.2. Determination of Rates

As the slope in the curve of $\ln OD_{600}$ as a function of time gives the growth rates of cells, natural logarithm of OD_{600} values were calculated to obtain specific growth rates by using the equation 2.1.

$$\mu = \frac{\Delta \ln OD_{600}}{\Delta t} \quad (2.1)$$

In order to determine uptake and secretion rates of the metabolites, the steady-state assumption is applied in three hours intervals as the shortest measured time-points. Missing data on cell dry weights are estimated from the OD_{600} values, and these cell dry weight data is used to calculate fluxes (in the unit of mmol/gDW_h). Measurement of the cell dry weight at the 3rd hour was crucial for the steady-state

assumption, however data was not available from the experiments. Curve trend of the OD₆₀₀ plot is used as a guide to estimate cell dry weight (Figure 2.1) **Need a method here: Estimation approach, maybe regression or curve fitting?**. Calculated flux values can be found in the Table 2.3.

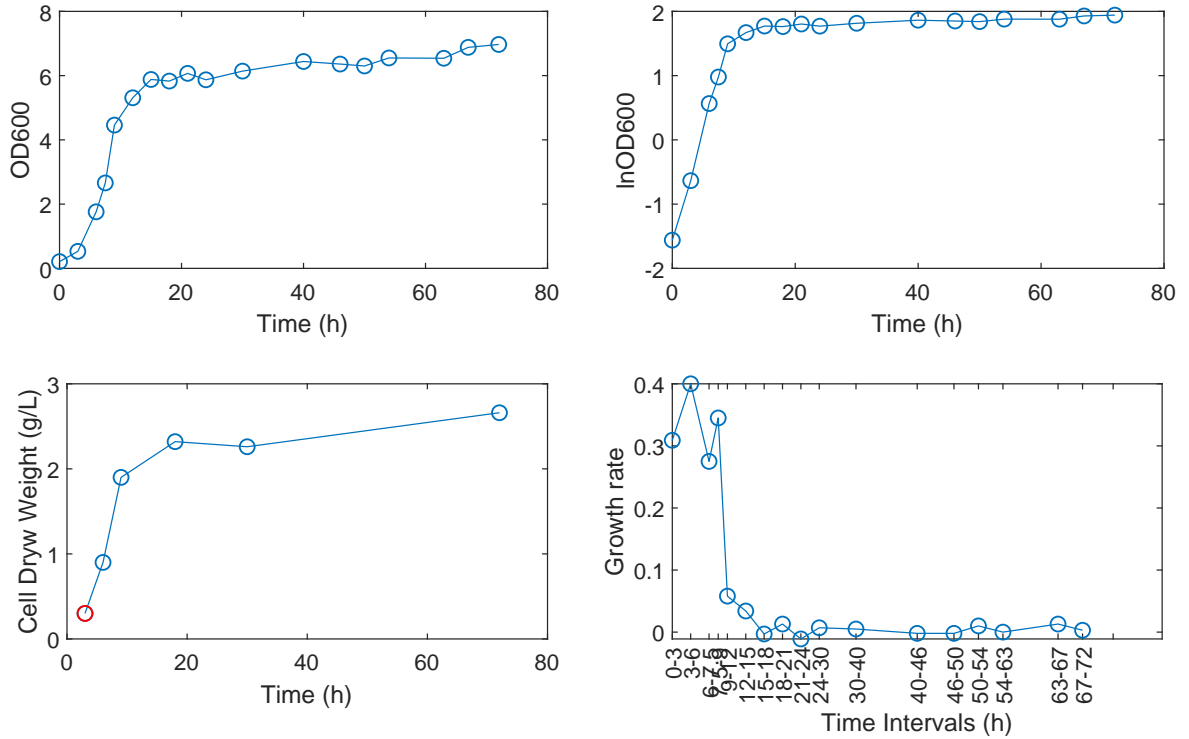


Figure 2.1. OD₆₀₀, lnOD₆₀₀, cell dry weights and growth rates graphs. Estimated missing cell dry weight data is shown in red color.

Table 2.3. Calculated flux values.

Time	Metabolite fluxes in mmol/gDWh				Growth h-1
	Glucose	Ethanol	Glycerol	Acetate	Biomass
0-3	-12.3963884	13.98837518	0.24131	2.960496	0.30859
3-6	-4.378823762	4.984363569	0.160873	-0.49342	0.400064

2.2. Model Selection

iAN50 [35], a stoichiometric model of intermediary metabolism including glycolysis, the pentose phosphate pathway (PPP), anaerobic excretion, citric acid cycle (TCA cycle), oxidative phosphorylation, and uptake pathways for galactose, ethanol and acetate is used to simulate batch conditions. The model was implemented based on the first GSMM of yeast, iFF708 [32] with the addition of the yeast intermediary metabolism from the RAVEN toolbox [36], and finally curated using the KEGG database [29].

Biomass equation (Eq. 2.2) in the model was left as a function of sub-reactions, for example protein, lipid, DNA synthesis reactions, so that the coefficients of biomass constituents could be optimized for each FBA simulation.

$$\begin{aligned}
 &0.5185 \text{ Glycogen} + 0.0234 \text{ Trehalose} + 0.8079 \text{ Mannan} + 1.1348 \text{ Glucan} \\
 &+ 0.1966 \text{ DNA} + 0.012 \text{ RNA} + 4.14 \text{ Protein} + 0.0269 \text{ Lipid} + 35.3630 \text{ Maintenance} \\
 &= \text{BIOMASS} \quad (2.2)
 \end{aligned}$$

Enzymatic reactions that are found in the model is collected in Table 2.4. In contrast to other GSMM's, each reaction was irreversible in the iAN50. This was achieved by splitting each reversible reaction into two separate reactions in both directions.

Another reason to select iAN50 is that the total masses of enzymes catalyzing reactions in the GSMM were already estimated, and fluxes through these reactions were constrained to the biologic level, using an approach similar to intracellular crowding method using kinetic parameters [37,38]. To clarify the method briefly, a flux value for each reaction was obtained by applying a standart flux balance analysis, and this value was divided by the maximum *in vitro* activity collected from the enzyme database BRENDA [39], and a saturation factor of 0.5 (half) for simplification. Therefore, the mass of the enzymes required for that particular reaction was estimated and the

constraints are applied to the corresponding enzymatic reactions.

Table 2.4. Reaction list in the iAN50 model.

NAME	EQUATION	GENE ASSOCIATION	EC-NUMBER	SUBSYSTEM
Hexokinase	$GLC[c] + ATP[c] \Rightarrow ADP[c] + G6P[c]$	YFR053C; YGL253W; YCL040W	2.7.1.1 OR 2.7.1.2	Glycolysis
Glucose-6-phosphate isomerase	$G6P[c] \rightleftharpoons F6P[c]$	YBR196C	5.3.1.9	Glycolysis
Phosphofructokinase	$ATP[c] + F6P[c] \Rightarrow ADP[c] + F16P[c]$	YGR240C; YMR205C	2.7.1.11	Glycolysis
Fructose-1,6-bisphosphatase	$F16P[c] \Rightarrow F6P[c] + P_i[c]$	YLR377C	3.1.3.11	Glycolysis
Fructose-bisphosphate aldolase	$F16P[c] \rightleftharpoons GA3P[c] + DHAP[c]$	YKL060C	4.1.2.13	Glycolysis
Triosephosphate isomerase	$DHAP[c] \rightleftharpoons GA3P[c]$	YDR050C	5.3.1.1	Glycolysis
Triosephosphate dehydrogenase	$GA3P[c] + NAD[c] + P_i[c] \rightleftharpoons P13G[c] + NADH[c]$	YJL052W; YJR009C; YGR192C	1.2.1.12	Glycolysis
Phosphoglycerate kinase	$P13G[c] + ADP[c] \rightleftharpoons P3G[c] + ATP[c]$	YCR012W	2.7.2.3	Glycolysis
Phosphoglycerate mutase	$P3G[c] \rightleftharpoons P2G[c]$	YKL152C; YDL021W; YOL056W	5.4.2.11	Glycolysis
Enolase	$P2G[c] \rightleftharpoons PEP[c]$	YGR254W; YHR174W; YOR393W; YPL281C; YMR323W	4.2.1.11	Glycolysis
Pyruvate kinase	$ADP[c] + PEP[c] \Rightarrow ATP[c] + PYR[c]$	YOR347C; YAL038W	2.7.1.40	Glycolysis
Glucose-6-phosphate 1-dehydrogenase	$G6P[c] + NADP[c] \Rightarrow G15L[c] + NADPH[c]$	YNL241C	1.1.1.49	Pentose Phosphate
6-phosphogluconolactonase	$G15L[c] \Rightarrow P6G[c]$	YNR034W; YCR073W-A; YHR163W; YGR248W	3.1.1.31	Pentose Phosphate
6-phosphogluconate dehydrogenase, decarboxylating	$P6G[c] + NADP[c] \Rightarrow CO2[c] + RU5P[c] + NADPH[c]$	YGR256W; YHR183W	1.1.1.44	Pentose Phosphate
ribose 5-phosphate isomerase	$RU5P[c] \rightleftharpoons R5P[c]$	YOR095C	5.3.1.6	Pentose Phosphate
Ribulose-phosphate 3-epimerase	$RU5P[c] \rightleftharpoons X5P[c]$	YJL121C	5.1.3.1	Pentose Phosphate
Transketolase	$R5P[c] + X5P[c] \rightleftharpoons GA3P[c] + S7P[c]$	YBR117C; YPR074C	2.2.1.1	Pentose Phosphate
Transaldolase	$GA3P[c] + S7P[c] \rightleftharpoons F6P[c] + E4P[c]$	YLR354C	2.2.1.2	Pentose Phosphate
Transketolase	$E4P[c] + X5P[c] \rightleftharpoons F6P[c] + GA3P[c]$	YBR117C; YPR074C	2.2.1.1	Pentose Phosphate
Pyruvate carboxylase 1	$ATP[c] + CO2[c] + PYR[c] \Rightarrow ADP[c] + OAA[c] + P_i[c]$	YGL062W; YBR218C	6.4.1.1	TCA
Citrate synthase, mitochondrial	$ACCOA[m] + OAA[m] \Rightarrow CIT[m] + COA[m]$	YNR001C; YPR001W	2.3.3.1	TCA
Aconitate hydratase, mitochondrial	$CIT[m] \rightleftharpoons ICI[m]$	YLR304C	4.2.1.3	TCA
Isocitrate dehydrogenase	$ICI[m] + NAD[m] \Rightarrow AKG[m] + CO2[m] + NADH[m]$	YNL037C; YOR136W	1.1.1.41	TCA
Isocitrate dehydrogenase [NADP], mitochondrial	$ICI[m] + NADP[m] \Rightarrow AKG[m] + CO2[m] + NADPH[m]$	YDL066W; YLR174W	1.1.1.42	TCA
Alpha-ketoglutarate dehydrogenase	$AKG[m] + NAD[m] + ADP[m] + P_i[m] \Rightarrow CO2[m] + NADH[m] + ATP[m] + SUC[m]$	YDR148C; YIL215W	1.2.4.2	TCA
Succinate dehydrogenase complex	$FAD[m] + SUC[m] \Rightarrow FADH2[m] + FUM[m]$	YKL148C; YLL041C	1.3.5.1	TCA
Fumarate reductase	$FADH2[m] + FUM[m] \Rightarrow FAD[m] + SUC[m]$	YJR051W; YEL047C	1.3.1.6	TCA
Fumarate hydratase	$FUM[m] \rightleftharpoons MAL[m]$	YPL262W	4.2.1.2	TCA
Malate dehydrogenase	$MAL[m] + NAD[m] \rightleftharpoons NADH[m] + OAA[m]$	YKL085W	1.1.1.37	TCA
Galactokinase	$GAL[c] + ATP[c] \Rightarrow GALP[c] + ADP[c]$		2.7.1.6	Galactose metabolism
UDP-glucose 4-epimerase	$GALUDP[c] \rightleftharpoons GLUUDP[c]$		5.1.3.2	Galactose metabolism
Galactose-1-phosphate uridylyltransferase	$GLUUDP[c] + GALP[c] \rightleftharpoons G1P[c] + GALUDP[c]$		2.7.7.12	Galactose metabolism
Phosphoglucomutase-1	$G1P[c] \rightleftharpoons G6P[c]$		5.4.2.2	Galactose metabolism
glycerol-3-phosphate dehydrogenase	$DHAP[c] + NADH[c] \Rightarrow GP[c] + NAD[c]$	YDL022W; YOL059W	1.1.1.8	Anaerobic excretion
sn-glycerol-3-phosphate phosphohydrolase	$GP[c] \Rightarrow GLY[c] + P_i[c]$	YER062C; YIL053W	3.1.3.21	Anaerobic excretion
Pyruvate decarboxylase	$PYR[c] \Rightarrow ACA[c] + CO2[c]$	YGR087C; YLR134W; YLR044C	4.1.1.1	Anaerobic excretion
Alcohol dehydrogenase	$ACA[c] + NADH[c] \rightleftharpoons ETH[c] + NAD[c]$	YGL256W; YMR303C; YOL086C	1.1.1.1	Anaerobic excretion
Aldehyde dehydrogenase	$ACA[c] + NADP[c] \Rightarrow AC[c] + NADPH[c]$	YPL061W	1.2.1.3	Anaerobic excretion
Aldehyde dehydrogenase [NAD(P)+] 1	$ACA[c] + NAD[c] \Rightarrow NADH[c] + AC[c]$	YMR170C; YMR169C; YOR374W; YOR374W; YER073W	1.2.1.5	Aromatic amino acid biosynthesis
Isocitrate lyase	$ICI[m] \Rightarrow Glyoxylate[m] + SUC[m]$	YER065C; YPR006C	4.1.3.1	Anaplerotic reactions
Malate synthase 1, glyoxysomal	$ACCOA[m] + Glyoxylate[m] \Rightarrow COA[m] + MAL[m]$	YIR031C; YNL117W	2.3.3.9	Anaplerotic reactions
NADH-ubiquinone oxidoreductase, mitochondrial ("Complex I")	$NADH[m] + Ubiquinone-9[m] \Rightarrow Ubiquinol[m] + NAD[m]$	YML120C; YMR145C	1.6.5.3 (1.6.5.9)	Oxidative Phosphorylation
External NADH-ubiquinone oxidoreductase 2, mitochondrial ("Complex I")	$NADH[c] + Ubiquinone-9[m] \Rightarrow Ubiquinol[m] + NAD[c]$	YDL085W	1.6.5.3 (1.6.5.9)	Oxidative Phosphorylation
Succinate dehydrogenase [ubiquinone] cytochrome b subunit, mitochondrial (Complex II)	$FADH2[m] + Ubiquinone-9[m] \rightleftharpoons FAD[m] + Ubiquinol[m]$	YKL141W; YDR178W	1.3.5.1	Oxidative Phosphorylation
Cytochrome b-c1 complex subunit Rieske, mitochondrial (complex III)	$Ubiquinol[m] + 2 \text{ Ferri}cytochrome_c[m] + 1.5 \text{ H}[m] \Rightarrow Ubiquinone-9[m] + 2 \text{ Ferri}cytochrome_c[m] + 1.5 \text{ HMit}[m]$	YEL024W; YBL045C; YHR001W-A; YPR191W; YFR033C; YDR529C; YJL166W; YGR183C	1.10.2.2	Oxidative Phosphorylation
Cytochrome c oxidase subunit 1 (Complex IV)	$Ferri cytochrome_c[m] + 0.25 \text{ O}_2[c] + 1.5 \text{ H}[m] \Rightarrow Ferri cytochrome_c[m] + 1.5 \text{ HMit}[m]$	YNL052W; YIL111W; YLR395C; Q0045; Q0250; YGL187C; YHR051W; YGL191W; YLR038C; YMR256C; YDL067C	1.9.3.1	Oxidative Phosphorylation
ATP synthase subunit alpha, mitochondrial (Complex V)	$ADP[m] + P_i[m] + 3 \text{ HMit}[m] \Rightarrow ATP[m] + 3 \text{ H}[m]$	YBL099W; Q0080; YPL078C; YDR298C; Q0130; Q0085; YJR121W; YKL016C; YDL004W; YDR322C-A; YPL271W; YDR377W; YPR020W; YBR039W; YLR295C; YML081C-A; YOL077W-A; YML042W	3.6.3.14	Oxidative Phosphorylation
ATP hydrolysis	$ATP[c] \Rightarrow ADP[c] + P_i[c]$			Other
Pyruvate dehydrogenase complex	$COA[m] + NAD[m] + PYR[m] \Rightarrow ACCOA[m] + CO2[m] + NADH[m]$	YER178W; YFL018C; YBR221C	1.2.4.1	Other
Acetyl-coenzyme A synthetase 1	$AC[c] + 2 \text{ ATP}[c] + COA[c] \Rightarrow ACCOA[c] + 2 \text{ ADP}[c] + 2 \text{ P}_i[c]$	YAL054C; YLR153C	6.2.1.1	Other
Phosphoenolpyruvate carboxykinase	$ATP[c] + OAA[c] \Rightarrow ADP[c] + CO2[c] + PEP[c]$	YKR097W	4.1.1.49	Other

2.3. Flux Balance Analysis

Uptake reaction of glucose with the secretion reactions of glycerol and acetate were constrained according to the calculated flux values in Table 2.3, for both time intervals separately. Since the main goal was to validate model for experimental conditions, ethanol was not constrained in regard to be used as the control metabolite. Experiments were done in fully aerobic conditions, therefore oxygen uptake reaction was set unlimited.

Coefficients of the biomass constituents are defined as the same as the batch conditions in the reference article [35], for the reason that detailed knowledge is not available in the acquired experimental data. Coefficients for the final biomass equation can be found in the Table 2.5.

Table 2.5. Biomass coefficients that are used in the simulation.

Constituent	Coefficient
Protein	3.703704
RNA	0.37037
DNA	0.018519
Lipid	0.041667
Glycogen	0.030864
Trehalose	0.029214
Mannan	0
Glucan	2.469136
Maintainance	40

For the linear optimization, an implementation of pFBA from the reference publication was performed [35, 40]. After solving the system using a linear solver with the objective maximizing growth, the solution was used as a constraint. From that point, a second optimization was run to minimize the sum of all other fluxes.

2.4. Visualization of the Model

The GSMM was visualized in Cytoscape [41] using the Fluxviz plug-in [42] and the solution fluxes were mapped onto edges. Network was imported in SBML [43] and the flux distributions were imported in csv format.

3. RESULTS

3.1. Intracellular Flux Distributions

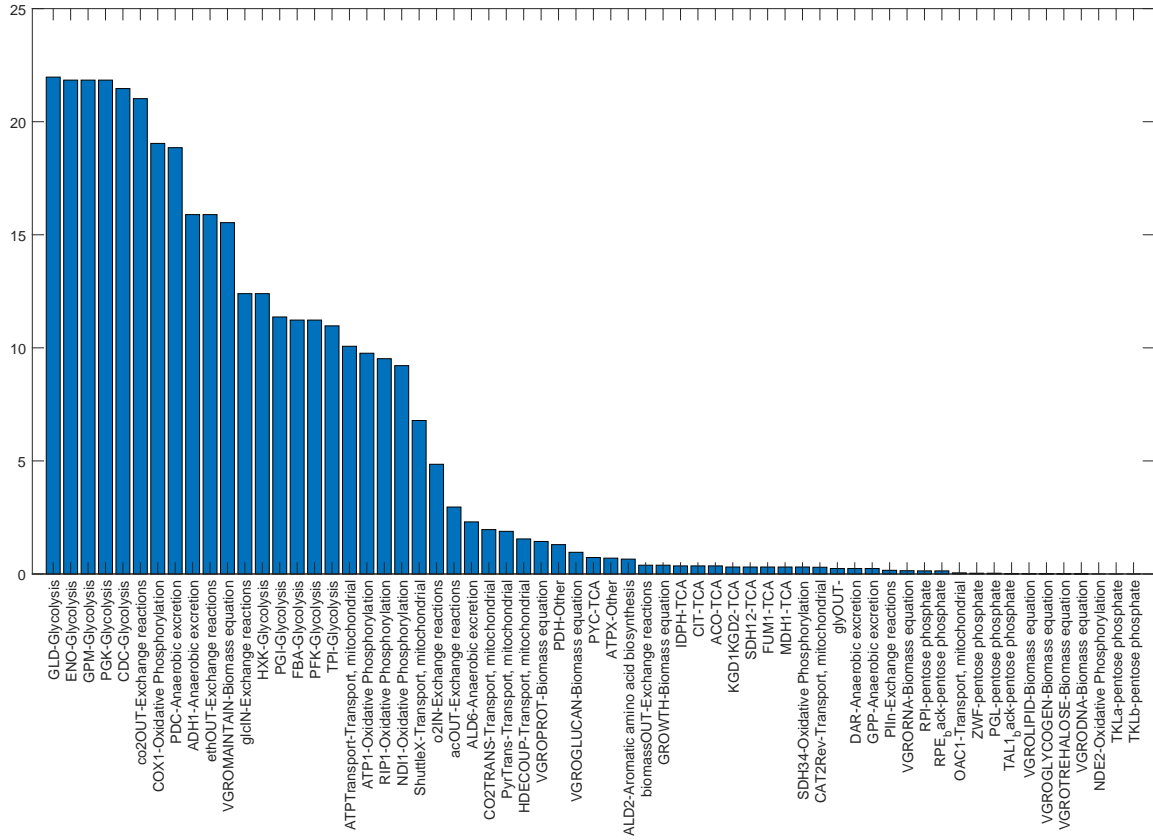


Figure 3.1. Non-zero fluxes in the solution.

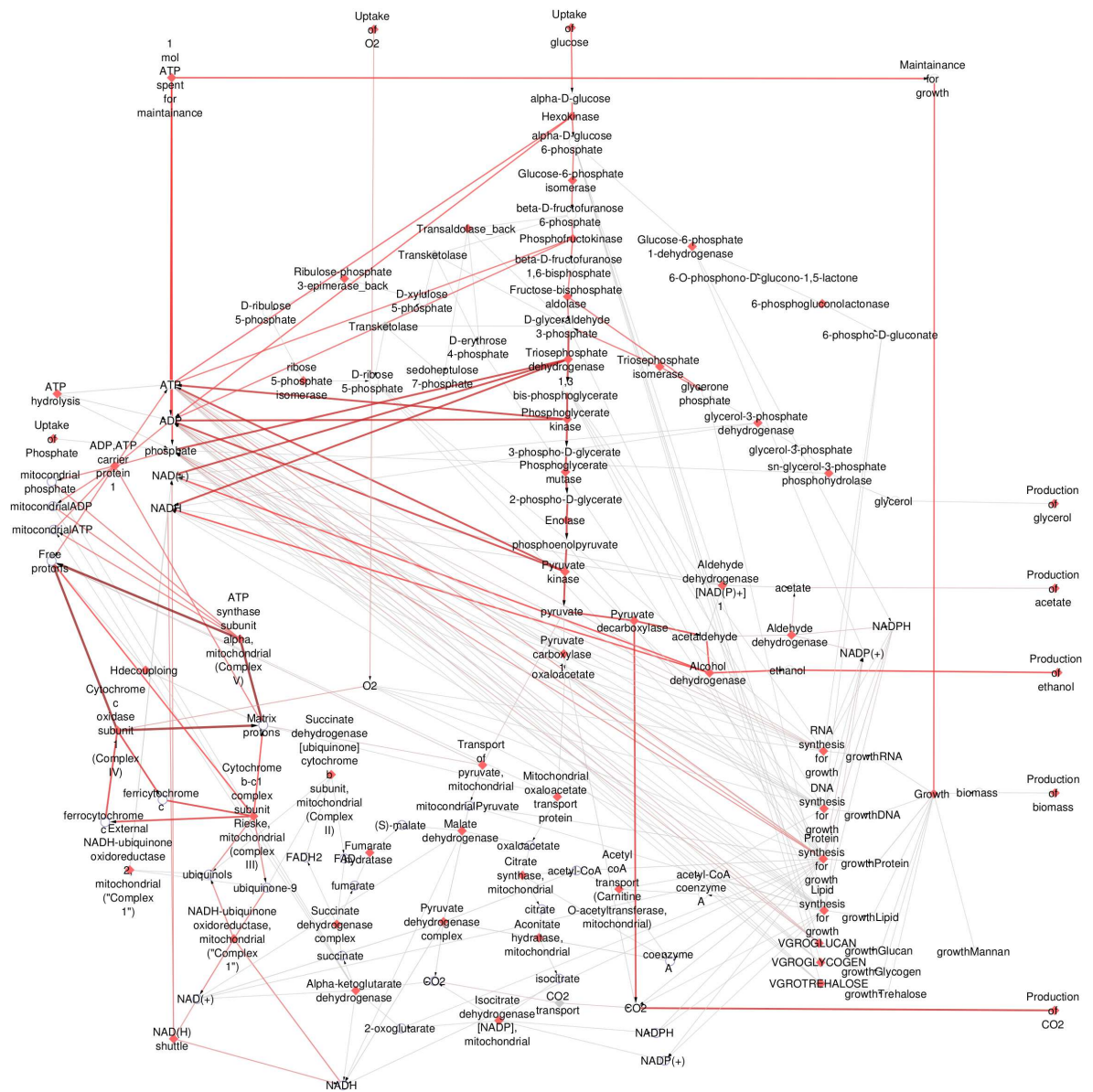


Figure 3.2. Non-zero flux distributions on the map.

4. DISCUSSION

5. EXPANDABLE TOPICS

5.1. Following topics can be added into introduction

Biological pathways (explaining each in detail, NAD regulation etc.), Fermentation (industrial applications, bio-ethanol, shift mechanisms in the yeast), Regulation Strategies in Cells (feedback/feedforward loops with figures), Toolboxes (such as COBRA, RAVEN or Other Softwares and Algorithms), FBA Methods (pFBA, dFBA, TFBA etc), Omics Data (subtopics for each omics, Model Integration Methods, maybe Transcriptomics Analysis if it is going to be used), Control analysis...

REFERENCES

1. Kitano, H., “Systems biology: a brief overview”, *science*, Vol. 295, No. 5560, pp. 1662–1664, 2002.
2. Bellouquid, A. and M. Delitala, *Mathematical modeling of complex biological systems*, Springer, 2006.
3. Kremling, A., *Systems biology: mathematical modeling and model analysis*, Chapman and Hall/CRC, 2013.
4. Bruggeman, F. J. and H. V. Westerhoff, “The nature of systems biology”, *TRENDS in Microbiology*, Vol. 15, No. 1, pp. 45–50, 2007.
5. Shahzad, K. and J. J. Loor, “Application of top-down and bottom-up systems approaches in ruminant physiology and metabolism”, *Current Genomics*, Vol. 13, No. 5, pp. 379–394, 2012.
6. Thiele, I. and B. Ø. Palsson, “A protocol for generating a high-quality genome-scale metabolic reconstruction”, *Nature protocols*, Vol. 5, No. 1, p. 93, 2010.
7. Orth, J. D., I. Thiele and B. Ø. Palsson, “What is flux balance analysis?”, *Nature biotechnology*, Vol. 28, No. 3, p. 245, 2010.
8. Vallino, J. J. and G. Stephanopoulos, “Carbon flux distributions at the glucose 6-phosphate branch point in *Corynebacterium glutamicum* during lysine overproduction”, *Biotechnology Progress*, Vol. 10, No. 3, pp. 327–334, 1994.
9. Varma, A., B. W. Boesch and B. O. Palsson, “Biochemical production capabilities of *Escherichia coli*”, *Biotechnology and bioengineering*, Vol. 42, No. 1, pp. 59–73, 1993.

10. Feist, A. M., M. J. Herrgård, I. Thiele, J. L. Reed and B. Ø. Palsson, “Reconstruction of biochemical networks in microorganisms”, *Nature Reviews Microbiology*, Vol. 7, No. 2, p. 129, 2009.
11. Pitkänen, E., P. Jouhten, J. Hou, M. F. Syed, P. Blomberg, J. Kludas, M. Oja, L. Holm, M. Penttilä, J. Rousu *et al.*, “Comparative genome-scale reconstruction of gapless metabolic networks for present and ancestral species”, *PLoS computational biology*, Vol. 10, No. 2, p. e1003465, 2014.
12. Kerkhoven, E. J., P.-J. Lahtvee and J. Nielsen, “Applications of computational modeling in metabolic engineering of yeast”, *FEMS Yeast Res*, Vol. 15, No. 1, pp. 1567–1364, 2014.
13. Chen, N., I. J. del Val, S. Kyriakopoulos, K. M. Polizzi and C. Kontoravdi, “Metabolic network reconstruction: advances in in silico interpretation of analytical information”, *Current opinion in biotechnology*, Vol. 23, No. 1, pp. 77–82, 2012.
14. Durot, M., P.-Y. Bourguignon and V. Schachter, “Genome-scale models of bacterial metabolism: reconstruction and applications”, *FEMS microbiology reviews*, Vol. 33, No. 1, pp. 164–190, 2008.
15. Dikicioglu, D., B. Kirdar and S. G. Oliver, “Biomass composition: the “elephant in the room” of metabolic modelling”, *Metabolomics*, Vol. 11, No. 6, pp. 1690–1701, 2015.
16. Machado, D. and M. Herrgård, “Systematic evaluation of methods for integration of transcriptomic data into constraint-based models of metabolism”, *PLoS computational biology*, Vol. 10, No. 4, p. e1003580, 2014.
17. Ramkrishna, D. and H.-S. Song, “Dynamic models of metabolism: Review of the cybernetic approach”, *AIChE Journal*, Vol. 58, No. 4, pp. 986–997, 2012.

18. Kim, T. Y., S. B. Sohn, Y. B. Kim, W. J. Kim and S. Y. Lee, “Recent advances in reconstruction and applications of genome-scale metabolic models”, *Current opinion in biotechnology*, Vol. 23, No. 4, pp. 617–623, 2012.
19. Stephanopoulos, G., “Metabolic fluxes and metabolic engineering”, *Metabolic engineering*, Vol. 1, No. 1, pp. 1–11, 1999.
20. Stephanopoulos, G., “Synthetic biology and metabolic engineering”, *ACS synthetic biology*, Vol. 1, No. 11, pp. 514–525, 2012.
21. Österlund, T., I. Nookaew and J. Nielsen, “Fifteen years of large scale metabolic modeling of yeast: developments and impacts”, *Biotechnology advances*, Vol. 30, No. 5, pp. 979–988, 2012.
22. Pinzon, W., H. Vega, J. Gonzalez and A. Pinzon, “Mathematical Framework Behind the Reconstruction and Analysis of Genome Scale Metabolic Models”, *Archives of Computational Methods in Engineering*, pp. 1–14, 2018.
23. Gélinas, P., “Inventions on baker’s yeast strains and specialty ingredients”, *Recent patents on food, nutrition & agriculture*, Vol. 1, No. 2, pp. 104–132, 2009.
24. Goffeau, A., J. Park, I. T. Paulsen, J.-L. JONNIAUX, T. Dinh, P. Mordant and M. H. SAIER JR, “Multidrug-resistant transport proteins in yeast: complete inventory and phylogenetic characterization of yeast open reading frames within the major facilitator superfamily”, *Yeast*, Vol. 13, No. 1, pp. 43–54, 1997.
25. Dujon, B., “The yeast genome project: what did we learn?”, *Trends in Genetics*, Vol. 12, No. 7, pp. 263–270, 1996.
26. Botstein, D., S. A. Chervitz and M. Cherry, “Yeast as a model organism”, *Science*, Vol. 277, No. 5330, pp. 1259–1260, 1997.
27. Barnett, J. A., “A history of research on yeasts 1: work by chemists and biologists

- 1789–1850”, *Yeast*, Vol. 14, No. 16, pp. 1439–1451, 1998.
28. Barnett, J. A., “A history of research on yeasts 2: Louis Pasteur and his contemporaries, 1850–1880”, *Yeast*, Vol. 16, No. 8, pp. 755–771, 2000.
 29. Kanehisa, M. and S. Goto, “KEGG: kyoto encyclopedia of genes and genomes”, *Nucleic acids research*, Vol. 28, No. 1, pp. 27–30, 2000.
 30. DeRisi, J. L., V. R. Iyer and P. O. Brown, “Exploring the metabolic and genetic control of gene expression on a genomic scale”, *Science*, Vol. 278, No. 5338, pp. 680–686, 1997.
 31. Cho, R. J., M. Fromont-Racine, L. Wodicka, B. Feierbach, T. Stearns, P. Legrain, D. J. Lockhart and R. W. Davis, “Parallel analysis of genetic selections using whole genome oligonucleotide arrays”, *Proceedings of the National Academy of Sciences*, Vol. 95, No. 7, pp. 3752–3757, 1998.
 32. Förster, J., I. Famili, P. Fu, B. Ø. Palsson and J. Nielsen, “Genome-scale reconstruction of the *Saccharomyces cerevisiae* metabolic network”, *Genome research*, Vol. 13, No. 2, pp. 244–253, 2003.
 33. Lopes, H. and I. Rocha, “Genome-scale modeling of yeast: chronology, applications and critical perspectives”, *FEMS yeast research*, Vol. 17, No. 5, 2017.
 34. Arslan, M., C. Holyavkin, H. İ. Kısakesen, A. Topaloğlu, Y. Sürmeli and Z. P. Çakar, “Physiological and transcriptomic analysis of a chronologically long-lived *Saccharomyces cerevisiae* strain obtained by evolutionary engineering”, *Molecular biotechnology*, Vol. 60, No. 7, pp. 468–484, 2018.
 35. Nilsson, A. and J. Nielsen, “Metabolic trade-offs in yeast are caused by F1F0-ATP synthase”, *Scientific reports*, Vol. 6, p. 22264, 2016.
 36. Agren, R., L. Liu, S. Shoaie, W. Vongsangnak, I. Nookaew and J. Nielsen, “The

- RAVEN toolbox and its use for generating a genome-scale metabolic model for *Penicillium chrysogenum*”, *PLoS computational biology*, Vol. 9, No. 3, p. e1002980, 2013.
37. Beg, Q. K., A. Vazquez, J. Ernst, M. A. de Menezes, Z. Bar-Joseph, A.-L. Barabási and Z. N. Oltvai, “Intracellular crowding defines the mode and sequence of substrate uptake by *Escherichia coli* and constrains its metabolic activity”, *Proceedings of the National Academy of Sciences*, Vol. 104, No. 31, pp. 12663–12668, 2007.
 38. Adadi, R., B. Volkmer, R. Milo, M. Heinemann and T. Shlomi, “Prediction of microbial growth rate versus biomass yield by a metabolic network with kinetic parameters”, *PLoS computational biology*, Vol. 8, No. 7, p. e1002575, 2012.
 39. Schomburg, I., A. Chang, S. Placzek, C. Söhngen, M. Rother, M. Lang, C. Munaretto, S. Ulas, M. Stelzer, A. Grote *et al.*, “BRENDA in 2013: integrated reactions, kinetic data, enzyme function data, improved disease classification: new options and contents in BRENDA”, *Nucleic acids research*, Vol. 41, No. D1, pp. D764–D772, 2012.
 40. Nilsson, A., “solveLinMin: Code of Implementation of pFBA”, GitHub, SysBioChalmers, EnzymeConstrainedSmallYeast, sourceCode, solveLinMin, 2019.
 41. Cline, M. S., M. Smoot, E. Cerami, A. Kuchinsky, N. Landys, C. Workman, R. Christmas, I. Avila-Campilo, M. Creech, B. Gross *et al.*, “Integration of biological networks and gene expression data using Cytoscape”, *Nature protocols*, Vol. 2, No. 10, p. 2366, 2007.
 42. König, M. and H.-G. Holzhütter, “Fluxviz—Cytoscape plug-in for visualization of flux distributions in networks”, *Genome Informatics 2010: Genome Informatics Series Vol. 24*, pp. 96–103, World Scientific, 2010.
 43. Hucka, M., F. T. Bergmann, A. Dräger, S. Hoops, S. M. Keating, N. Le Novère, C. J. Myers, B. G. Olivier, S. Sahle, J. C. Schaff *et al.*, “The Systems Biology

Markup Language (SBML): language specification for level 3 version 2 core”, *Journal of integrative bioinformatics*, Vol. 15, No. 1, 2018.